*European Cells and Materials* Vol.58 2026 (pages 214–229) DOI: 10.22203/eCM.v058a15 ISSN 1473-2262

*Original Article*

# *Atractylodes Macrocephala Koidz.* Derived Exosome-Like Nanovesicles Promoted Osteogenic Differentiation of hBMSCs Via Regulating SOD2 and Postponed Osteoporosis of Ovariectomized Rats

Ziquan Zhao[1,†], Zhina Peng[2,†], Weixiong Guo[1], Xuyang Wu[1], Zhuolan Zhong[1], Tianyi Hu[2], Xinqia Huang[1], Mingzhu Deng[1], Weiqiang Zhan[1] and Jiaqi Chu[2,3,*]

[1]Orthopaedic Center, Affiliated Hospital of Guangdong Medical University, 524001 Zhanjiang, Guangdong, China
[2]Department of Obstetrics and Gynecology, Affiliated Hospital of Guangdong Medical University, 524001 Zhanjiang, Guangdong, China
[3]Stem Cell Research and Cellular Therapy Center, Affiliated Hospital of Guangdong Medical University, 524001 Zhanjiang, Guangdong, China
[†]These authors contributed equally.

**Abstract**

**Objective**: Osteoporosis is a chronic disease associated with decreased bone strength and a heightened susceptibility to fractures. *Atractylodes macrocephala Koidz.* (AMK) is a traditional Chinese herb that tonifies the spleen and invigorates qi, which helps to strengthen muscles and bones. In this study, AMK-derived exosome-like nanovesicles (AMKELNs) are studied to determine whether they function in osteogenic differentiation of human bone marrow-derived mesenchymal stem cells (hBMSCs) and in osteoporosis of ovariectomized (OVX) rats. **Methods**: AMKELNs were extracted from the rhizome of AMK by differential centrifugation, whose structure was visualized by transmission electron microscopy, and the particle size was determined by nanoparticle tracking analysis. A series of experiments, such as quantitative reverse transcription polymerase chain reaction (qRT-PCR), western blot, alkaline phosphatase (ALP) activity, and alizarin red staining, were conducted to evaluate the effect of AMKELNs on osteogenic differentiation of hBMSCs. Furthermore, AMKELNs were intraperitoneally injected into OVX rats for 12 weeks of treatment. Micro computed tomography (Micro-CT) and histological staining were performed to assess the effects of AMKELNs on osteoporosis. **Results**: AMKELNs with an intact bilayer membrane and an average size of 141.9 $\pm$ 0.5 nm were successfully internalized by hBMSCs and absorbed by Sprague-Dawley rats. Moreover, AMKELNs stimulated the osteogenic differentiation of hBMSCs by up-regulating the expression of superoxide dismutase 2 (SOD2). In the animal experiment (n = 5), AMKELNs could effectively preserve the bone mass of rats and improve the bone parameters. **Conclusions**: Our results indicate that AMKELNs represent a promising therapeutic method for osteoporosis. This study proposes a new theoretical perspective on bone tissue repair strategies based on a natural drug nano-delivery system.

**Keywords:** *Atractylodes macrocephala Koidz.*, SOD2, exosome-like nanovesicles, hBMSCs, osteoporosis.

***Address for correspondence**: Jiaqi Chu, Department of Obstetrics and Gynecology, Affiliated Hospital of Guangdong Medical University, 524001 Zhanjiang, Guangdong, China; Stem Cell Research and Cellular Therapy Center, Affiliated Hospital of Guangdong Medical University, 524001 Zhanjiang, Guangdong, China. E-mail: chujiaqi@gdmu.edu.cn.



## Introduction

Osteoporosis is one of the prevalent diseases that cause significant social and economic burdens [1]. Osteoporosis is a chronic disease characterized by reduced bone density. The decrease in bone mass disrupts the bone microstructure, making it more prone to fragility [2]. Therefore, osteoporosis is a key target for preventing fractures [3]. Specifically, drugs have been developed to inhibit bone resorption, for instance, bisphosphonates [4]; or stimulate bone formation, such as Teriparatide [5]. Human bone marrow mesenchymal stem cells (hBMSCs) have a talent for osteogenic differentiation and contribute to bone formation [6,7]. Despite these advances, due to rare side effects and underestimation of the fracture risk, the gap in osteoporosis treatment options is currently growing. New drugs with longer-lasting efficacy and higher patient acceptance need to be developed to improve this situation [8].

Plant-derived exosome-like nanovesicles (PELNs) have gained attention as a promising strategy for tissue repair and anti-aging research [9]. With nanoscale membrane structures, they can transport a lot of genetic information and metabolites. These components are transferred between different species and can regulate the biological

functions of organisms [10]. What's more, PELNs are minimally cytotoxic to healthy tissues, biocompatible, and capable of tumor targeting through specific endocytosis mechanisms [11]. So far, PELNs have exerted numerous therapeutic effects in cardiotoxicity improvement [12], liver protection [13], lung injury repair [14], digestive tract anti-inflammation [15], etc. PELNs are heterogeneous vesicles, having different sources and exerting unique functions: the original cells often carry cell-specific products and may promote cellular recovery and maintain internal environment homeostasis, thereby initiating bone repair and regeneration [16].

*Atractylodes macrocephala Koidz.* (AMK) is a perennial herb of the genus *Atractylodes* in the family *Compositae* [17]. It exhibits pharmacological activities including spleen-strengthening, qi-tonifying, dampness-drying, diuretic, anti-hyperhidrotic, and pregnancy-stabilizing effects [18]. The rhizome is the medicinal parts, possessing anti-inflammatory, antioxidant, and immune-enhancing effects [19]. Drawing on the concept of traditional Chinese medicine, spleen-strengthening is believed to facilitate nutrient assimilation, support renal health, and enhance bone and muscle strength. Previous studies have shown that the active components or extracts of AMK serve an essential function in orthopedics [20–23]. For example, Atractylenolide I mitigated glucocorticoid-induced osteoporosis by targeting the Nuclear factor kappa-light-chain-enhancer of activated B cells (NF-$\kappa$B) signaling pathway [24], indicating that AMK also possesses the potential for preventing osteoporosis. Based on these findings, AMK has been proposed as a natural drug that can regulate bone mass [25].

Superoxide dismutases (SODs) are a family of superoxide dismutase enzymes [26] and are mainly divided into superoxide dismutase 1 (SOD1) (located in the cytoplasm), superoxide dismutase 2 (SOD2) (localized in the mitochondrial matrix), and superoxide dismutase 3 (SOD3) (present in the extracellular matrix). These enzymes establish the first line of resistance to reactive oxygen species (ROS) via stimulating the dismutation of superoxide anion radicals, which are then converted into hydrogen peroxide and water. Accordingly, SODs function as crucial antioxidants, shielding cells from oxidative stress and ultimately preserving cellular viability [27]. What's more, SODs have been confirmed to have the ability to enhance osteogenic differentiation of stromal cells [28]. For instance, SOD2, a superoxide dismutase, could clear ROS by increasing the phosphorylation level of Smad3 in human periodontal ligament stem cells, positively regulating the gene and protein expression of alkaline phosphatase (ALP), bone morphogenetic protein 6 (BMP6), and RUNX family transcription factor 2 (Runx2), and achieving the effect of regulating osteogenic differentiation [29].

The principal objective of the present study is to validate the influence of AMK-derived exosome-like nanovesicles (AMKELNs), on the osteogenic differentiation of hBMSCs, as well as the role of the key factor SOD2 in this process. Besides, by conducting an *in vivo* experiment on the effect of AMKELNs in preventing bone loss in rat models of postmenopausal osteoporosis (PMOP), this study may provide some useful insight into osteoporosis from bench to bedside.

## Materials and Methods

### *Isolation and Characterization of AMKELNs*

Extraction of AMKELNs was carried out via differential centrifugation. Briefly, the fresh and cleaned AMK (originating from Lishui, Zhejiang, China) was soaked in phosphate buffered saline (PBS) (w/v, 1:5) and pulsed until chopped. The supernatant was obtained after centrifugation at 1500 × g for 30 minutes and 12,000 × g for 1 hour, which removed contaminants and cell remnants. Subsequently, the sample was subjected to ultracentrifugation at 100,000 × g for 70 minutes in an ultracentrifuge (Optima XPN-100, Beckman Coulter Inc., Brea, CA, USA). The sediment was resuspended with sterile PBS and subsequently filtered through a 0.22 $\mu$m filter membrane. The samples obtained were AMKELNs. Protein concentrations were determined using a BCA assay kit (GenStar E162-01, China). The spare AMKELNs were stored at –80°C until further use. To visualize the vesicular structures, AMKELNs were supported by nickel grids and stained with 1% uranyl acetate. A transmission electron microscope (TEM) (JEM-1200EX, JEOL Ltd., Tokyo, Japan) was used to photograph the morphological structure of AMKELNs. The particle size was evaluated by Nanoparticle Tracking Analysis (NTA) using a NanoSight NS300 instrument (Malvern Panalytical, Malvern Worcestershire, England).

### *Isolation and Culture of hBMSCs*

Bone marrow samples acquired from female patients aged 60 to 65 years undergoing hip replacement surgery were collected and utilized for BMSC extraction. All procedures were conducted in accordance with the Declaration of Helsinki and were approved by the Medical Ethical Committee of the Affiliated Hospital of Guangdong Medical University (Zhanjiang, Guangdong, China). The primary BMSCs were isolated with the help of Histopaque-1077 (10771, Sigma-Aldrich, Product of UK). The samples were centrifuged at 400 × g for 20 minutes to be separated based on density. The cells in the middle layer were collected and seeded into a culture flask with MEM-Alpha (C12571500BT, Gibco, Made in China) complete medium supplemented with 10% (v/v) fetal bovine serum (FBS), 100 U/mL penicillin G and 100 $\mu$g/mL streptomycin (all purchased from Gibco, Thermo Fisher Scientific, Inc, 10099-141C originating from Australia, 15140122 originating from USA). The obtained hBMSCs were cultured in a humidified incubator at 37°C with 5% $CO_2$ until they adhered. The medium was replaced at 3-day intervals. Once the cell confluence reached approximately 90%, hBMSCs

were trypsinized (25200072, Gibco, Made in Canada) and split at a ratio of 1:3 for subculture. Cells from the 4th to 7th generations were utilized for subsequent experiments.

*Detection of Mycoplasma During the Culture of hBMSCs*

To eliminate the influence of mycoplasma on this experiment, the supernatants during cell culture were collected for testing. The following experiments were performed according to the corresponding manual.

According to the instruction of MycoBlue Mycoplasma Detector (D101, Vazyme, China), the supernatant from 72 hours after the cell culture was added to the working solution containing MycoBlue Enzyme. The same volume of PBS served as a negative control. The reaction tubes were incubated at a constant temperature of 60°C for 60 minutes. The results were visually compared by the color of the mixture. The solution shows sky blue for positive or purple for negative of mycoplasma.

Another way was performed as stated in the manual of Myco-Lumi$^{TM}$ Luminescent Mycoplasma Detection Kit (C0297S, Beyotime, China). The supernatants from different passages of hBMSCs were collected and centrifuged at 400 $\times$ g for 5 minutes. 50 $\mu$L of the upper liquid from each sample was dispensed into individual wells of a white 96-well plate. Reagent A was subsequently added for reaction, and the mixture was incubated at 20–25°C. After 5 minutes, chemiluminescence detection was carried out via Synergy H1 microplate reader (BioTek Instruments, Inc., Winooski, VT, USA), and the reading value was A. Subsequently, reagent B was introduced into each well and incubated at 20–25°C for 10 minutes. In the same way, the reading value was recorded as B. The ratio B/A of each sample was calculated. A ratio higher than 1.2 indicates the presence of mycoplasma contamination. However, if less than 0.9, it indicates a negative result.

*Phenotype of hBMSCs*

Flow cytometry was employed to identify the phenotype of hBMSCs. The P4 hBMSCs were digested when they reached 80% confluence, centrifuged at 200 $\times$ g for 3 minutes, and redispersed. The Human Mesenchymal Stem Cell Analysis Kit (562245, BD Biosciences, USA) was used to detect the expression of the surface markers, such as the cluster of differentiation 73, 90, 105, 34, 11b, 19, and the human leukocyte antigen-DR isotype (CD73, CD90, CD105, CD34, CD11b, CD19, HLA-DR). The processed cells were analyzed on a FACSCanto II flow cytometry system (BD Biosciences, Ashland, OR, USA) following the manufacturer's protocols, and the data were processed with FlowJo software (Version v10.8.1, BD Biosciences, Ashland, OR, USA).

*Multilineage Differentiation of hBMSCs*

The hBMSCs were seeded in 12-well plates at a density of 5 $\times$ $10^4$ cells per well. 24 hours later, hBMSCs started to be cultured in osteogenic-induced medium (OIM, Low-glucose Dulbecco's Modified Eagle Medium (C11885500BT, Gibco, Made in China) supplemented with 100 nM dexamethasone, 50 $\mu$M L-ascorbic acid-2-phosphate, 10 mM $\beta$-glycerophosphate (D4902, A8960, G9422; all purchased from Sigma-Aldrich, Merck KGaA, USA), and 10% FBS). As for adipogenic differentiation, the cells were treated with adipogenesis induction medium (AIM, High-glucose Dulbecco's Modified Eagle Medium (C11995500BT, Gibco, Made in China) supplemented with 10% FBS, 500 nM dexamethasone, 10 $\mu$g/mL insulin, 500 $\mu$M 3-Isobutyl-1-methylxanthine and 50 $\mu$M indomethacin (I5500, I5879, I7378; purchased from Sigma-Aldrich, USA)). Each induction medium was refreshed at 3-day intervals throughout the 14-day induction period. The hBMSCs were fixed with 4% paraformaldehyde (BL539A, Biosharp, China) for 15 minutes and stained with Alizarin red or Oil Red O (ALIR-10001, OILR-10001; all purchased from Oricell, Cyagen Biosciences, Guangzhou Inc, China) for 15 minutes. Images were captured under a microscope.

For the chondrogenic differentiation experiment, hBMSCs at a density of 2 $\times$ $10^5$ cells/mL were centrifuged in a 15 mL tube at 200 $\times$ g for 3 minutes. After incubation at 37°C for 1 day, the cells settled and aggregated into small spheres. The medium was then substituted with chondrogenic induction medium (CIM, containing MEM-Alpha minimum essential medium (C12571500BT, Gibco, Made in China), 1% FBS, 10 ng/mL TGF-$\beta$ (PeproTech 100-21C, America), 1% insulin-transferrin-selenium (Gibco$^{TM}$41400045, America), 5 $\mu$g/mL L-ascorbic acid-2-phosphate and 20 nM dexamethasone). The CIM was replaced at 3-day intervals throughout the 21-day induction period. The hBMSCs spheres were fixed with 4% paraformaldehyde, dehydrated under a gradient, embedded in paraffin, and sectioned. The slides were stained with Alcian Blue. Images were captured under a microscope.

*Internalization of AMKELNs*

AMKELNs were labeled with PKH26 (MINI26-1KT, Sigma-Aldrich, USA). Generally, AMKELNs were treated with 500 $\mu$L diluted C solution combined with 4 $\mu$L PKH26 dye solution and shielded from light and maintained at ambient temperature for 20 minutes. After incubation, 500 $\mu$L exosome-free FBS was applied to terminate the reaction. The samples were ultracentrifuge at 110,000 $\times$ g for 70 minutes, and the PKH26-labeled AMKELNs (PKH26-AMKELNs) were resuspended in sterile PBS. These labeled AMKELNs were co-cultured with hBMSCs on cell slides for 24 hours. Subsequently, the cell slides were fixed with 4% paraformaldehyde, permeabilized with 0.1% Triton X-100 (T6200G, Biotopped, China) in PBS (PBST) for 20 minutes, and blocked with 1% bovine serum albumin (BSA) (A8020, Solarbio, China) at room temperature for 1 hour. To visualize the cytoskeletal protein structure, the samples were sequentially treated with $\alpha$-Tubulin primary

antibody and Alexa Fluor 488-conjugated secondary antibody for 1 hour each. The nuclei were stained with DAPI (H-1200, Vector Laboratories, USA). The images were photographed using an LSM900 device (Zeiss, Oberkochen, Baden-Württemberg, Germany).

*Cell Proliferation Assay*

The effect of AMKELNs on hBMSCs viabilities was assessed by Cell Counting Kit-8 (K009, Zeta Life, USA). Briefly, hBMSCs were seeded in 96-well plates at a density of 3000 cells per well and subjected to AMKELNs at increasing concentrations (0, 1, 5, 10, 20, 40 and 80 $\mu$g/mL) for 24, 48 and 72 hours. Upon completion of incubation, CCK-8 working solution was introduced into each well, and the plates were incubated at 37°C for 1 hour. The absorbance at 450 nm was measured via Synergy H1 microplate reader and Gen5 CHS 3.05 software (BioTek Instruments, Inc., Winooski, VT, USA).

*Osteogenic Differentiation Assay*

hBMSCs were seeded in 12-well plates at a density of $5 \times 10^4$ cells per well. When the confluence reached over 80%, the cells were induced for osteogenic differentiation. The experimental groups were cultured in OIM supplemented with 1, 5, 10, or 20 $\mu$g/mL AMKELNs, while the control group was cultured with OIM only.

On the 6th day of induction, the expression of ALP was detected. Cells were fixed with 4% paraformaldehyde for 15 minutes, washed with PBS to remove residual fixative. The expression of alkaline phosphatase was detected using a BCIP/NBT Chromogen Kit (PR1100, Solarbio, China).

Around the 12th day of induction, alizarin red staining was conducted for the sake of evaluating the mineral deposition of hBMSCs. For specific steps, please refer to the section entitled "Multilineage Differentiation of hBMSCs". The results were observed visually and microscopically (Olympus BX53, Evident, Tokyo, Japan).

For comparison, the positively stained area of five non-repeating fields from each well was quantified using ImageJ (Version 1.53c, National Institutes of Health, Bethesda, MD, USA).

*Total RNA Extraction and Quantitative Reverse Transcription Polymerase Chain Reaction (qRT-PCR)*

hBMSCs were seeded in a 6-well plate for adherent culture. After 5 days of induction, total RNA was extracted from hBMSCs using NucleoZOL (740404.200, MN, Germany). Genomic DNA removal and reverse transcription into cDNA were executed in accordance with the manual of HiScript III RT SuperMix reagent (R323-01, Vazyme, China). Further, ChamQ Universal SYBR qPCR Master Mix (Q711-02, Vazyme, China) was applied to qPCR reactions. The data were obtained by QuantStudio Dx and QuantStudio Test Development Software v1.0.1 (Thermo Fisher Scientific, Carlsbad, CA, USA). The mRNA expressions of the osteogenic-related genes were normalized to those of the internal control ($\beta$-actin) and quantified using the $2^{-\Delta\Delta Ct}$ method. The primer sequences were designed (listed in Table 1) and custom-synthesized by Sangon Biotech Company (Shanghai, China).

*Western Blot*

After 12 days of induction, cells were lysed with RIPA buffer (89900, Invitrogen, USA). Protein concentration was determined using a BCA protein assay kit. Equal amounts of protein (20 $\mu$g) from each group were loaded onto 10% or 12% SDS-PAGE gels for separation and subsequently electrotransferred onto PVDF membranes (ISEQ00010, Merck Millipore, USA). The membranes were then blocked with 5% skim milk at room temperature for 1–2 hours. Then they were treated with primary antibodies (listed in **Supplementary Table 1**) overnight and maintained at 4°C. The membranes were washed three times with Tris-buffered saline with Tween-20 (TBST, T1085, Solarbio, China), then the incubation with fluorescence-labelled secondary antibodies was performed with protection from light for 1 hour. The membranes were washed three times, with a 10-minute interval between each wash. The visualization and fluorescence intensity detection of the proteins were achieved by the Odyssey® CLX dual-color infrared laser imaging system and Image Studio Ver 5.2 software (both from LI-COR Biotechnology, Lincoln, NE, USA).

*Eukaryotic Transcriptomics Analysis with Reference*

Osteogenic-induced hBMSCs were treated with AMKELNs or PBS, and RNA samples were prepared. RNA-sequencing was performed on the Illumina platform by Guangzhou New Gene Biotechnology Co., Ltd. (Guangdong, China). The main steps were as follows: RNA extraction, enrichment, and rRNA removal. After concentration and detection of purity and integrity, the samples were qualified for library construction to obtain corresponding gene sequence information and to perform data alignment analysis. Hierarchical Clustering was used to obtain the overall clustering results of the samples. Genes exhibiting a $|\log2 \text{ Fold change}| \geq 1$ and an adjusted $p$ value less than 0.05 were considered differentially expressed genes (DEGs). The volcano plot was drawn to visualize the trend of gene expression changes. The data were analyzed and exported with R 4.3.3 (R Foundation for Statistical Computing, Vienna, Austria).

*Cell Transfection Experiment*

The siRNA sequence targeted to SOD2 was designed and synthesized by Synbio Technologies (Suzhou, Jiangsu, China). The sense (5′-3′) sequence was CACGCUUACUACCUUCAGUdTdT, and the antisense (5′-3′) sequence was ACUGAAGGUAGUAAGCGUGdTdT. The siSOD2 sequence was transfected into hBMSCs using

**Table 1. Sequences of primers for qPCR.**

| Species | Gene | Forward sequence (5′ to 3′) | Reverse sequence (5′ to 3′) |
|---|---|---|---|
| Human | *ALP* | CTTCAAACCGAGATACAAGCACTC | CGTTGTTCCTGTTCAGCTCGTAC |
| | *Runx2* | CTCTACTATGGCACTTCGTCAGG | TCAGCGTCAACACCATCATTC |
| | *OCN* | GAGGGCAGCGAGGTAGTGAA | TAGACCGGGCCGTAGAAGC |
| | *OPN* | GGGAAGGACAGTTATGAAACGAG | CCTGACTATCAATCACATCGGAAT |
| | *β-actin* | CACCATTGGCAATGAGCGGTTC | AGGTCTTTGCGGATGTCCACGT |
| | *SOD2* | TAGCTCTTCAGCCTGCACTG | CAGCAACTCCCCTTTGGGTT |

Lipofectamine™ RNAiMAX (13778150, Thermo Fisher Scientific Inc., Carlsbad, CA, USA). The transfection lasted for 24 hours, and then the culture medium was substituted for either proliferation or differentiation. Cell samples were collected at the corresponding time points for further experimentation.

*Distribution of AMKELNs in SD Rats*

As instructed by the manual, a 5 mM DiR (D12731, Thermo Fisher Scientific, Inc, USA) staining solution was prepared and applied to label AMKELNs. The mixture with a final concentration of 5 $\mu$M was incubated at ambient temperature for 30 minutes. After incubation, the mixture was transferred to an ultracentrifuge tube containing PBS and centrifuged at 110,000 × g for 70 minutes at 4°C under vacuum pumping. The supernatant was discarded, and the precipitate was dissolved in PBS. The DiR-labeled AMKELNs (DiR-AMKELNs) were filtered and intraperitoneally injected into Sprague-Dawley (SD) rats, with each receiving 500 $\mu$g of AMKELNs. 24 hours later, the main organs of the rats (heart, liver, spleen, lung, kidneys, humeri and femurs) were collected. The distribution of DiR-AMKELNs in the rats was observed using the AniView100 multi-mode imaging system (BioLight Biotechnology, Guangzhou, Guangdong, China).

*Animal Experiment*

All experiments adhered to the Chinese Law on Laboratory Animal Welfare (Guideline for Ethical Review of Animal Welfare, Standard number: GB/T 35892–2018) and the National Institutes of Health Guide for the Care and Use of Laboratory Animals. The animal experiment was approved by the Experimental Animal Ethics Committee of the Affiliated Hospital of Guangdong Medical University (Approval No. AHGDMU-LAC-B-202405-0024). A total of 15 female Sprague-Dawley (SD) rats (7–8 weeks, weighing approximately 200–220 g) were purchased from SPF (Beijing) Biotechnology Co., Ltd. (China), and were quality-tested by Suzhou Xishan Biotechnology Co., Ltd. (Jiangsu, China). The rats were randomly caged in the SPF-level barrier environment of the Experimental Animal Center of the Affiliated Hospital of Guangdong Medical University and were fed with standard nutritional pellet feed and had free access to water. After one week of adaptive feeding, they were used for the formal experiment.

The animals were randomly allocated into three groups (n = 5): sham-operated rats with ovaries intact and peri-ovarian fat removed only (Sham group), bilaterally ovariectomized (OVX) rats (OVX group), and OVX rats treated with 1 mg/kg AMKELNs (OVX + AMKELNs group). Bilateral ovariectomy was performed on rats to establish a PMOP model. AMKELNs were administered intraperitoneally every week during the following 12 weeks. There was a continuous measurement of body weight of each group. The animals were eventually euthanized using inhalational anesthetics combined with cervical dislocation. Samples from both femurs, along with the heart, liver, spleen, lung, and kidneys, were collected and immersed in 4% paraformaldehyde for 72 hours. The fixative was then washed off and replaced with 75% ethanol for long-term preservation. The animal carcasses were uniformly disposed of by the hospital's medical waste treatment center.

*Micro Computed Tomography (Micro-CT) Scanning and Analysis*

The femur images were scanned via SCANCO vivaCT80 (pixel size 8.82 $\mu$m, working voltage 70 kV, current 114 $\mu$A, power 8 W, exposure time 220 ms; SCANCO Medical AG, Brüttisellen, Switzerland). The CTAn software (Version 1.18.4.0, Bruker MicroCT, Billerica, MA, USA) was used to analyze a total of 120 slices, with each voxel size 15.6 $\mu$m. To better understand the trabecular bone structure, the following parameters were calculated: bone mineral density (BMD, g/mm$^3$), bone volume (BV, mm$^3$), bone volume fraction (BV/TV, %), trabecular number (Tb.N, 1/mm), trabecular pattern factor (Tb.Pf, 1/mm), and structure model index (SMI, 1).

*Histology and Immunohistochemistry (IHC)*

The fixed femur tissues were decalcified in 12% EDTA-$Na_2$ solution (pH 7.35–7.45, E8030, Solarbio, China) for 6 weeks. Thereafter, the decalcified tissues were paraffin-embedded and serially-sectioned at 5 $\mu$m. Prior to staining, slides were subjected to xylene and a descending series of ethanol solutions for dewaxing and rehydration. After washing with PBS, a rapid antigen retrieval solution (P0090, Beyotime, China) was utilized for antigen retrieval. The bone sections were blocked for endogenous peroxidase activity and nonspecific binding, and then covered with Runx2 or osteocalcin (OCN) primary antibod-

ies. Subsequently, they were incubated with streptavidin-conjugated secondary antibody for 1 hour and developed with 3,3′-diaminobenzidine (DAB-1031, Fuzhou Maixin Biotech Co., Ltd., China). Eventually, they were counterstained with hematoxylin and mounted. The images were acquired via an Olympus Ix73 microscope (Evident, Japan).

In addition, the femur sections were respectively stained with Hematoxylin & Eosin (H&E) and Masson's trichrome staining, referring to the instructions (G1120 and G1346, Solarbio, China). H&E staining was also performed on various organs of the rats to evaluate the biocompatibility of AMKELNs.

*Statistics*

Data analysis was conducted using GraphPad 9.5.0 (GraphPad Software, LLC, Boston, MA, USA). Results are expressed as the mean ± standard deviation of three independent replicates. The Student's t-test was used for comparisons between two groups, and one-way ANOVA was used for comparisons among multiple groups. Statistical significance was defined as a $p$-value less than 0.05 ($p < 0.05$).

## Results

*Extraction and Characterization of AMKELNs*

AMKELNs were extracted from fresh AMK by differential centrifugation (Fig. 1**a**). The pictures obtained from TEM revealed that AMKELNs exhibited the characteristic cup-shaped vesicular morphology with an intact bilayer membrane (Fig. 1**b**). The NTA report showed that the average particle size distribution of AMKELNs was 141.9 ± 0.5 nm, most of which was 115.9 ± 5.5 nm (Fig. 1**c**). It was estimated that there were approximately 30 mg AMKELNs within 15 mL PBS extracted from 1 kg AMK. The proportion was about $2.395 \times 10^{12} \pm 3.13 \times 10^{11}$ particles/mL (data not shown).

*AMKELNs Could be Internalized into hBMSCs*

With a strong capacity to differentiate into osteoblasts, BMSCs are regarded as optimal seed cells for bone tissue engineering. The active constituents of natural PELNs mainly serve their biological functions intracellularly. Therefore, it is crucial for AMKELNs to be absorbed into hBMSCs.

First and foremost, the collected cells were labeled and classified. hBMSCs were characterized by flow cytometry based on their specific surface markers. As shown in **Supplementary Fig. 1g**, more than 95% of hBMSCs were positive for CD73, CD90 and CD105. Meanwhile, only 1.76% of the cells expressed the negative markers comprising CD19, CD34, CD11b, CD45 and HLA-DR. During the proliferation culture, the cells were in good condition (**Supplementary Fig. 1a**), and there was no evidence of mycoplasma contamination (**Supplementary Fig. 1b–c**). Additionally, the cells were treated with different staining solutions to identify their osteogenic differentiation ability, the adipogenic differentiation ability, and the chondrogenic differentiation ability, respectively (**Supplementary Fig. 1d–f**). To prove whether AMKELNs could be taken up by hBMSCs, PKH26 was used to label AMKELNs. As shown in Fig. 1**d**, PKH26-labeled AMKELNs (red fluorescence) were primarily distributed in the cytoplasm around the nucleus, and some of them were also inside the nucleus. These results indicated that AMKELNs were successfully internalized by hBMSCs within 24 hours.

*AMKELNs Have no Evident Inhibitory Effect on the Proliferation of hBMSCs*

Given that AMKELNs contained a large number of bioactive components [30], a CCK-8 assay was performed to assess their proliferative activity on hBMSCs. After co-culturing AMKELNs with hBMSCs for 24 hours, 48 hours and 72 hours, it could be inferred that there was no obvious cytotoxicity on hBMSCs from the results (Fig. 2**a**).

*AMKELNs Promote Osteogenic Differentiation of hBMSCs*

To further investigate the osteogenic differentiation abilities of hBMSCs induced by AMKELNs, the following experiments were conducted within a safe concentration range according to the CCK-8 assay. It could be observed that within the increasing concentration from 1 μg/mL to 20 μg/mL, AMKELNs promoted the expression of alkaline phosphatase and the formation of mineralized nodules, as manifested by the gradually enhanced staining intensity of BCIP/NBT substrate (Fig. 2**c**, 2**e**) and alizarin red staining (Fig. 2**d**, 2**f**). Further research revealed that during the osteogenic induction in hBMSCs, the gene expressions of osteogenic-related markers Runx2, OCN, and osteopontin (OPN) were evidently increased (Fig. 2**h**), and the expressions of osteogenic-related proteins ALP, Runx2, and OPN were also markedly improved (Fig. 2**b**, 2**g**). These findings indicate that AMKELNs exert a beneficial effect on the osteogenic differentiation of hBMSCs.

*AMKELNs upregulate the expression of SOD2 in hBMSCs*

To further investigate how AMKELNs regulate the osteogenic differentiation of the hBMSCs, a transcriptome sequencing analysis was conducted. After treating the hBMSCs with 10 μg/mL AMKELNs for osteogenic induction for 5 days, the total RNA was collected, and the changes in gene expression levels were statistically analyzed, as shown in Fig. 3. Combining the outcomes of the fold changes and $p$ values, it could be inferred that 372 groups of genes changed significantly, among which 300 groups of genes were upregulated, and 72 groups of genes were downregulated (Fig. 3**a**). The heatmap (Fig. 3**b**) shows the expression variation of the differentially expressed genes. The volcano plot (Fig. 3**c**) revealed that compared to other genes, the expression of SOD2 was more prominent. There-

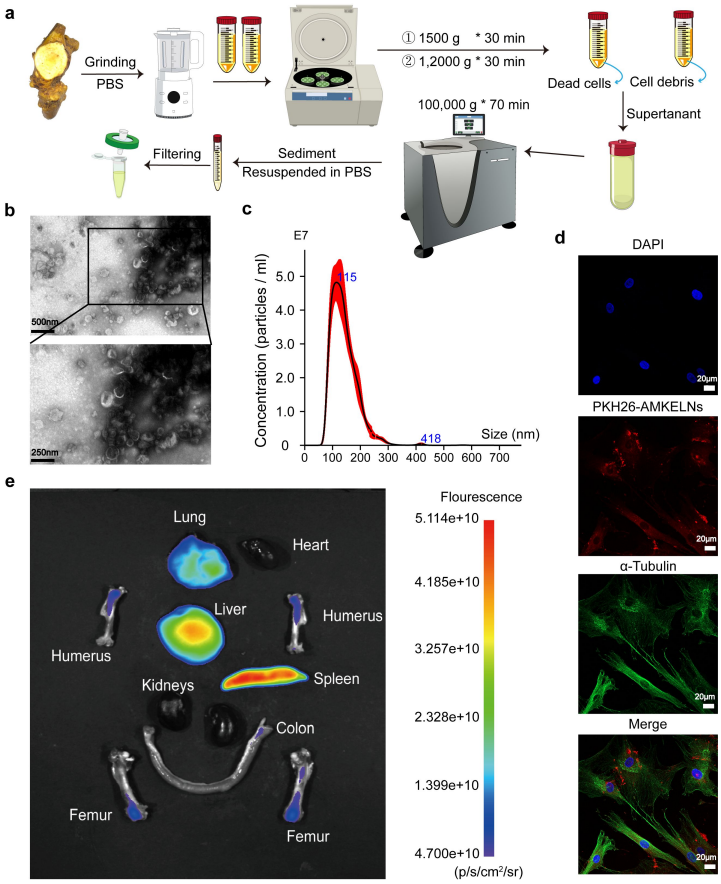


**Fig. 1. Extraction and Characterization of AMKELNs.** (**a**) Isolate AMKELNs with PBS from the rhizome part of AMK by differential centrifugation. (**b**) The structural morphology of AMKELNs captured by TEM. (**c**) Measurement of particle size for AMKELNs by NTA. (**d**) Internalization of PKH26-labeled AMKELNs (red) into hBMSCs. hBMSCs were revealed by DAPI-stained nuclei (blue) and $\alpha$-Tubulin-labeled cytoskeleton (green) (Scale bar = 20 $\mu$m). (**e**) Images of the colon, heart, lung, liver, spleen, kidneys, humeri and femurs were captured 24 hours after intraperitoneal injection (i.p.) of DiR-labeled AMKELNs to assess the biodistribution in SD rats. Fluorescence intensity unit: p/s/cm$^2$/sr. PBS, phosphate buffered saline; AMKELNs, AMK-derived exosome-like nanovesicles. The figure was designed and assembled with the assistance of Adobe Illustrator 2023 (Version 27.0.1).

fore, it could be reasonably hypothesized that SOD2 might be critical for AMKELNs-induced hBMSCs to differentiate into osteoblasts.

To further study whether SOD2 contributed to osteogenic differentiation, the mRNA expression and the protein level of SOD2 were detected and shown in Fig. 3**h** and **j**. The results indicated that in the presence of 10 $\mu$g/mL AMKELNs, SOD2 expression at both mRNA and protein levels was enhanced in hBMSCs. Therefore, a specific siRNA was synthesized to knock down the mRNA expression of SOD2. Consequently, the mRNA expression of ALP was decreased (Fig. 3**i**), and the protein levels of ALP and OPN were also significantly decreased. Additionally, the staining results in the later stages revealed that the expression of ALP (Fig. 3**d**, 3**f**) and the formation of mineralized nodules (Fig. 3**e**, 3**g**) were decreased, indicating that the osteogenic differentiation of hBMSCs was inhibited. However, in hBMSCs transfected with the siSOD2 sequence, treatment with 10 $\mu$g/mL AMKELNs restored the expression of ALP and OPN proteins (Fig. 3**j**, 3**k**). The ALP activity and the deposition of mineralized nodules increased as well, yet the staining intensities were not as good as those of the negative control group (NC). Therefore, these findings suggest that AMKELNs can improve the osteogenic differentiation of hBMSCs by dramatically up-regulating the expression of SOD2.

### *AMKELNs Prevented Bone Loss Induced by OVX*

To observe the biodistribution of AMKELNs *in vivo*, DiR-labeled AMKELNs were injected into SD rats. As shown in Fig. 1**e**, 24 hours after intraperitoneal injection, DiR-AMKELNs accumulated in the humeri and the femurs. Beyond that, a large amount of fluorescence signal could be observed in the liver and the spleen, while the content in the kidneys was relatively low. These observations suggest that the intraperitoneally injected AMKELNs can be absorbed into the systemic circulation and targeted to the bone tissues.

To investigate the therapeutic efficacy of AMKELNs

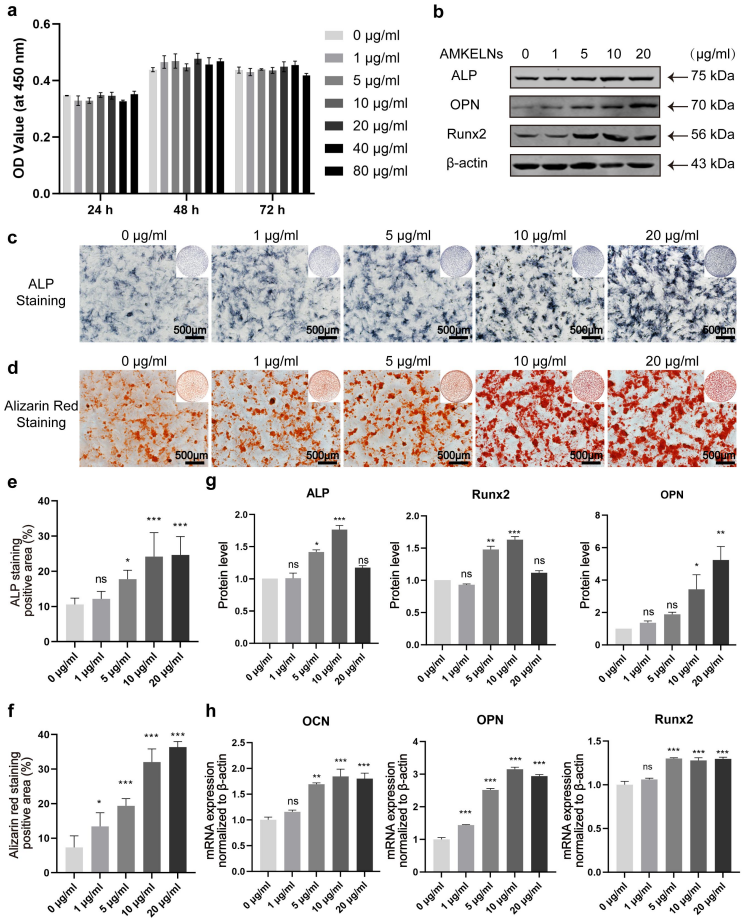


**Fig. 2. AMKELNs stimulate the osteogenic differentiation abilities of hBMSCs.** (**a**) CCK-8 assay was performed to assess the effect of escalating concentrations of AMKELNs (0, 1, 5, 10, 20, 40 and 80 $\mu$g/mL) on hBMSCs proliferation at 24, 48 and 72 hours. (**b**) Western Blot was used to analyze the protein levels of ALP, Runx2 and OPN in AMKELNs-induced hBMSCs after 12 days. (**c–f**) ALP expressions and the deposition of mineralized nodules were utilized to evaluate the osteogenic differentiation of AMKELNs-induced hBMSCs. Respectively, BCIP/NBT staining was performed on the 5th day (**c**) and alizarin red staining on the 12th day (**d**) of induction (Scale bar = 500 $\mu$m). The positive area fraction (**e** and **f**) was evaluated by the ImageJ software. (**g**) Quantitative analysis of each protein normalized to the loading control. (**h**) qRT-PCR analysis of gene expressions of Runx2, OCN and OPN in AMKELNs-induced hBMSCs compared with the control group (0 $\mu$g/mL) after 5 days of osteogenic differentiation. (n = 3, $^{*}p < 0.05$, $^{**}p < 0.01$, $^{***}p < 0.001$, and *ns* represents not significant.). AMKELNs, AMK-derived exosome-like nanovesicles; ALP, alkaline phosphatase; OPN, osteopontin; Runx2, RUNX family transcription factor 2; OCN, osteocalcin; OD, Optical Density. The images were plotted using GraphPad Prism 9.5.0 and assembled and annotated using Adobe Illustrator 2023 (Version 27.0.1).

on postmenopausal osteoporosis, OVX rat models were established. The rats were injected with AMKELNs once a week at a dosage of 1 mg/kg for 12 weeks (Fig. 4**a**). During this process, the weight changes of each group of rats were regularly monitored. It can be observed that the body weight of the OVX rats had increased by 140.8 ± 24.61 g, apparently more than the Sham group (76 ± 12.45 g). This phenomenon might be attributed to estrogen deficiency, which was helpful to confirm the effect of ovarian removal from another perspective. In the meantime, the body weight changes of the treatment group (OVX + AMKELNs) were intermediate between those of the other two groups (Fig. 4**b**).

With treatments finished, the femurs of rats (n = 5) were isolated for Micro-CT scanning, and the parameters of the trabecular bone were analyzed (Fig. 4**c**). Compared with the distal femur from the Sham group, the trabecular structure of the OVX group was extensively damaged. What's more, the BMD, BV, BV/TV (%), and Tb.N of the OVX rats decreased distinctly ($p < 0.001$). Nevertheless, the Tb.Pf and SMI of the OVX group were increased, indicating that the trabeculae changed from plate-like to a rod-like structure. Thus, the OVX model was successful in terms of bone loss. Surprisingly, 1 mg/kg of AMKELNs could reverse the trabecular structure disorder caused by bilateral ovariectomy. The BMD, BV, and BV/TV (%) in the treatment group (OVX + AMKELNs) were superior to those in the OVX group. Meanwhile, AMKELNs treat-

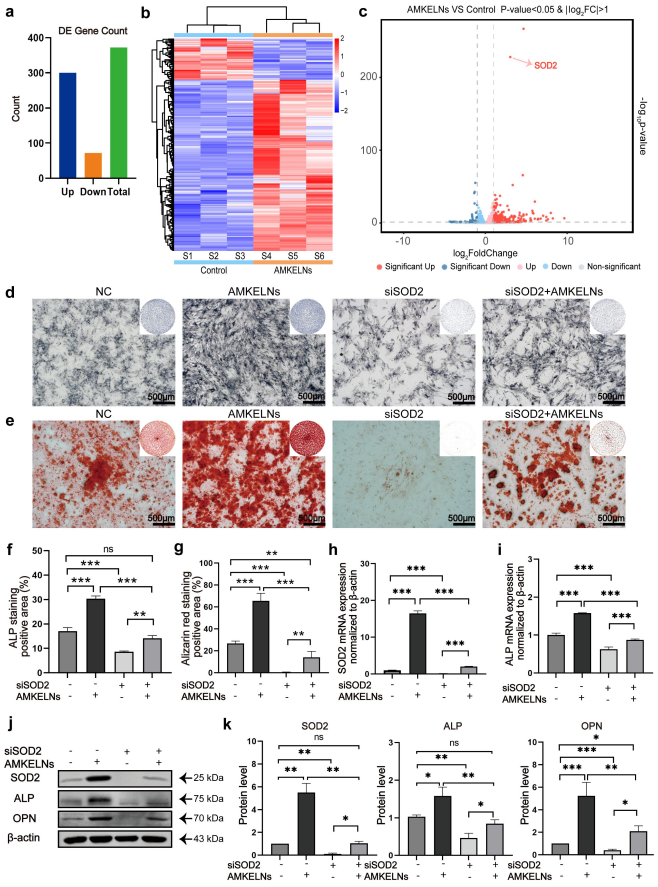


**Fig. 3. AMKELNs facilitate hBMSCs' osteogenesis by increasing SOD2 expression.** (**a**) Histogram of DEGs identified by cell transcriptomics sequencing analysis. (**b**) Heatmap comparing the expression of gene expression profiles between the control and AMKELNs-induced groups (drawn with R 4.3.3). (**c**) Volcano plot served to visualize the DEGs between the control and AMKELNs-induced groups (drawn with R 4.3.3). (**d**) BCIP/NBT staining and (**e**) Alizarin red staining and the relevant analysis (**f** and **g**) by ImageJ software were conducted respectively on hBMSCs treated with siSOD2-transfection or AMKELNs (Scale bar = 500 $\mu$m). qRT-PCR was performed to assess the mRNA expression of SOD2 (**h**) and ALP (**i**) at day 5 of hBMSCs osteogenic differentiation after the transfection with siSOD2 to knock down the mRNA expression of SOD2. (**j**) Western Blot and (**k**) relevant quantitative analysis were conducted to estimate the protein levels in hBMSCs after 12 days (n = 3, $^{*}p < 0.05$, $^{**}p < 0.01$, $^{***}p < 0.001$, and *ns* represents not significant.). NC, control group; AMKELNs, AMK-derived exosome-like nanovesicles; SOD2, superoxide dismutase 2; ALP, alkaline phosphatase; OPN, osteopontin. The images were plotted by GraphPad Prism 9.5.0 and were assembled using Adobe Illustrator 2023 (Version 27.0.1).

ment led to a decrease in Tb.Pf and SMI. In contrast to the Sham group, OVX rats possessed a damaged trabecular bone structure as shown in H&E staining (Fig. 5). In addition, the expression of Runx2 in bone marrow cells and OCN in bone matrix was badly decreased, as well as the production of bone collagen fibers according to Masson staining. However, these situations could be improved with AMKELNs treatment.

In conclusion, these results contribute to illustrating the positive role of AMKELNs on bone mass retention in OVX rats.

### *Biological Safety of AMKELNs in Vivo*

To evaluate the pharmacological and toxicological properties of AMKELNs, the heart, lung, liver, spleen, and kidney were isolated for further study. From H&E staining, it was clear that there were no significant signs of damage observed in these major organs (Fig. 6). There was little typical infiltration of inflammatory cells. This indicates that continuous intraperitoneal administration of AMKELNs is relatively safe for the organism.

## Discussion

Bone regeneration in osteoporosis is facing both opportunities and challenges [31]. Osteoporosis is a common degenerative bone disease caused by disrupted bone metabolism, pathologically featuring the disturbances of the balance between osteoblast-mediated bone formation and osteoclast-mediated bone resorption [32]. Postmenopausal osteoporosis (PMOP) is a prevalent disease associated with aging and estrogen deficiency. It can cause an imbalance in both fat metabolism and hormonal home-

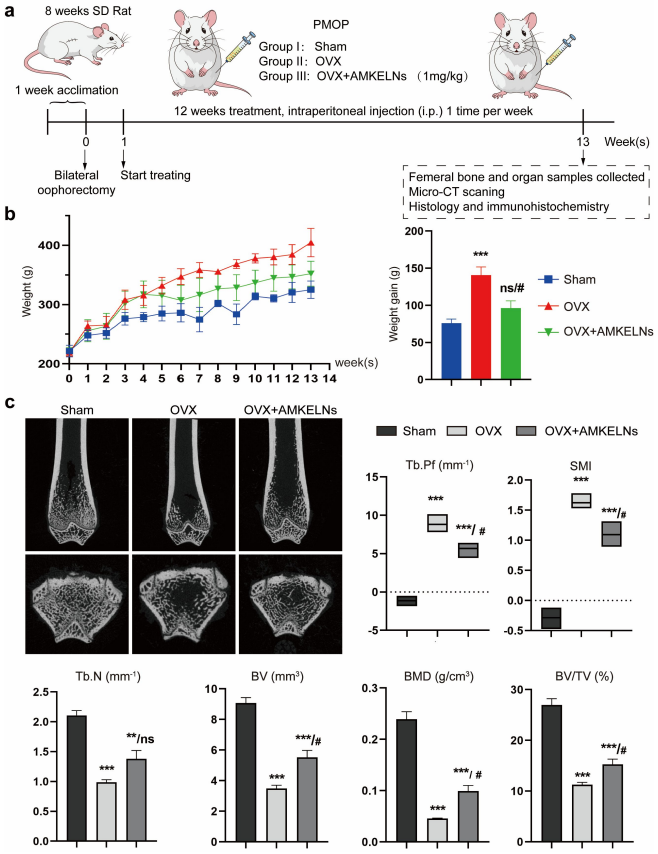


**Fig. 4. AMKELNs postpone the reduction in bone mass of OVX rats.** (**a**) Schematic diagram of experimental procedures in animals. Female rats underwent bilateral OVX or sham surgery. Intraperitoneal injections of AMKELNs were administered every week for 12 weeks. Then the rats were sacrificed. The figure was designed and assembled with the assistance of Adobe Illustrator 2023 (Version 27.0.1). (**b**) Tendency of body weight changes observed in the animals during the experiment. (**c**) Micro-CT was employed to evaluate the bone microarchitecture in each group. Top, sagittal plane; Bottom, transverse axis. The relevant bone parameters were analyzed to evaluate the function of AMKELNs in preventing osteoporosis. PMOP, postmenopausal osteoporosis; OVX, ovariectomized; AMKELNs, AMK-derived exosome-like nanovesicles; BMD, bone mineral density; BV, bone volume; BV/TV, bone volume fraction (bone volume/total volume); Tb.N, number of trabeculae; Tb.Pf, trabecular pattern factor; SMI, structural model index. Data are presented as mean ± SD (n = 5). $^{*}$, compared with the Sham group; $^{\#}$, compared with the OVX group. $^{**}p < 0.01$, $^{***}p < 0.001$, $^{\#}p < 0.05$, and ns represents not significant. The images were plotted by GraphPad Prism 9.5.0 and were assembled using Adobe Illustrator 2023 (Version 27.0.1).

ostasis [33,34], resulting in weight changes (Fig. 4**b**). At the same time, the lack of estrogen leads to the activation of NF-$\kappa$B signaling [35], which disrupts the bone balance between bone resorption and bone remodeling. Stem cell therapy is popular due to its great capability in bone regeneration and repair, with osteoporosis as a primary therapeutic target [36]. The process of MSCs differentiating into osteoblasts can be helpful to stabilize the balance. In our studies, a novel therapeutic potential of AMKELNs provided a reference for the prophylaxis and therapy of osteoporosis, which could improve the osteogenic activity of hBMSCs and delay the progression of bone loss in OVX rats.

PELNs have turned into a new strategy for regulating bone homeostasis [37]. PELNs derived from various plants, such as *Yam* [38], *Pueraria lobata* [39], and *Rhizoma Drynariae* [40], have shown therapeutic potential for osteoporosis. This bioactivity is likely related to their known pharmacological properties, since these herbs are traditionally used in Chinese medicine to strengthen tendons and tonify bones. Moreover, beyond these direct effects, the regulation of liver and spleen function is also believed to promote kidney nourishment and support musculoskeletal health [41]. This study started with the spleen-strengthening AMK, presented a new osteogenic differentiation stimulator targeting SOD2 from another perspective, and demonstrated the feasibility of AMKELNs in preventing and treating osteoporosis.

The main function of AMK is to strengthen the spleen and invigorate qi. It is reported that it can play an important role in anti-inflammation, antioxidation, and anticancer. However, there are few studies about its application in bone-related diseases. Nevertheless, it can be noticed

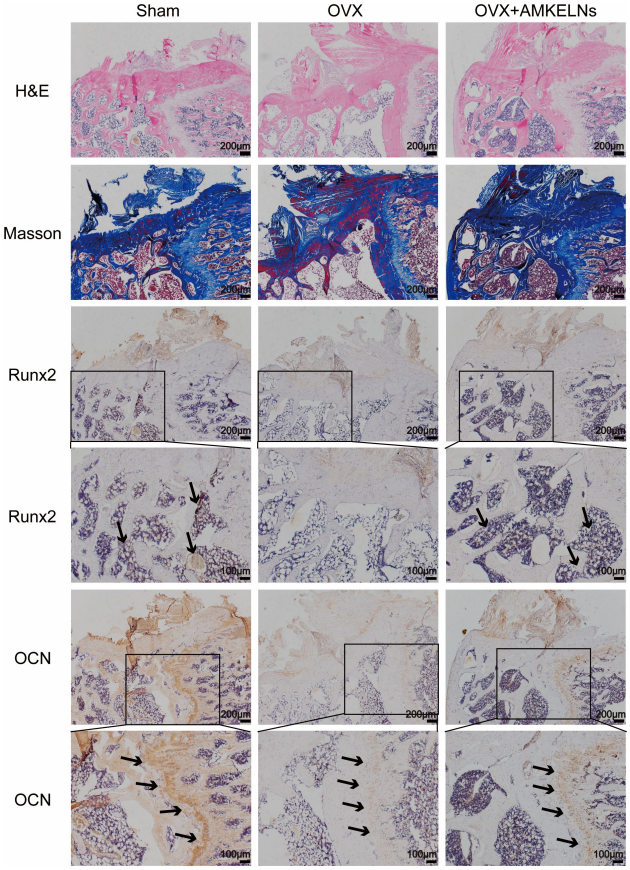


**Fig. 5. The histological staining results on the femurs of each group.** To evaluate the bone microstructure of femurs in each group, femur sections were subjected to H&E staining for bone microstructure, Masson staining for collagen fibers, and IHC for Runx2 and OCN protein expressions. OVX, ovariectomized; AMKELNs, AMK-derived exosome-like nanovesicles; H&E, Hematoxylin & Eosin; Runx2, RUNX family transcription factor 2; OCN, osteocalcin. The figure was assembled and annotated using Adobe Illustrator 2023 (Version 27.0.1).

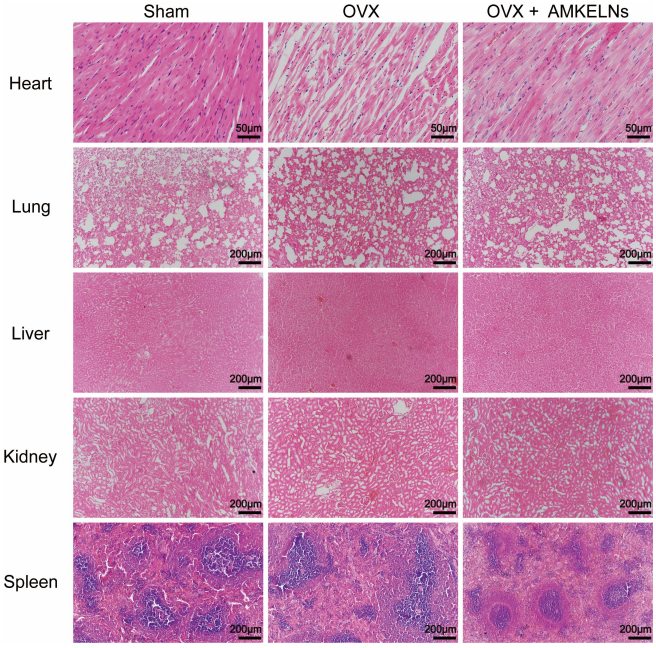


**Fig. 6. *In vivo* toxicity of AMKELNs.** H&E staining of tissues such as heart, lung, liver, kidney, and spleen after i.p. of AMKELNs or PBS (as a control) for 12 weeks. OVX, ovariectomized; AMKELNs, AMK-derived exosome-like nanovesicles. The figure was assembled and annotated using Adobe Illustrator 2023 (Version 27.0.1).

that some previous studies combined AMK with other traditional Chinese medicines for the treatment of osteoporosis [42,43]. Based on these, it can be supposed that AMK would have the potential to prevent osteoporosis. Lee *et al*. [44] found that the ethanol extract of AMK could suppress the osteoclast differentiation of RAW264.7 cells, which is a key event in the pathogenesis of osteoporosis. Meanwhile, they confirmed that the extract contained antioxidant components such as phenolic substances, flavonoids, and anthocyanins. However, there are still no relevant reports on whether AMK or its active components can postpone osteoporosis *in vivo*. In our experiments, AMKELNs accumulated in bone tissue and lessened bone loss in OVX rats, an effect associated with enhanced collagen fiber formation and sustained expression of Runx2 and OCN.

Transcriptomics analysis of cells indicated that AMKELNs-induced hBMSCs could enhance osteogenic activity via the up-regulated expression of SOD2. An increasing number of studies have shown that SOD2 contributes to the antioxidant stress response, which prevents cells from undergoing various forms of death [27], such as ferroptosis [45,46]. Further research has demonstrated that SOD2 deficiency in the osteoblast lineage induced an osteoporotic feature in the murine model [47]. SOD2 could be deacetylated at K68 by sirtuin 3 and thus influenced the mitochondrial stress to maintain osteoblast differentiation [48]. However, these manifestations have not yet been revealed in hBMSCs. Li *et al*. [49] found that under the circumstance of inflammation induced by TNF-$\alpha$, human adipose-derived MSCs, with the promotion of glycolysis and the reduced level of mitochondrial reactive oxygen species (mtROS) by SOD2, could exert immunomodulatory functions while their adipogenic differentiation was inhibited as an adaptive response. The adipogenic differentiation and osteogenic differentiation of stem cells are mutually restrictive [50,51], and the disruption of this balance may result in osteoporosis [52,53].

Unlike the previous reports [29,48,54], our results demonstrated that SOD2 could also function in mesenchymal stem cells from bone marrow. What counts is that there is a large demand for energy during the osteogenic differentiation of BMSCs. To cope with this change, the major energy supply mode of hBMSCs shifts from glycolysis to oxidative phosphorylation in mitochondria [55]. Oxidative phosphorylation is an unstable state and involves electron transport between oxidized and reduced molecules during energy production. It inevitably generates reactive oxygen species (ROS), for example, superoxide anion and hydroxyl radicals [56]. Therefore, cells produce antioxidant enzymes such as catalase, glutathione peroxidase, and superoxide dismutase, to scavenge free radicals and protect cellular membranes from oxidative damage [57]. SOD2 (MnSOD), as one of the superoxide dismutases, is the mitochondrial antioxidant that exists as a homotetramer and is located in the mitochondrial matrix [58]. Figures in our experiments showed that AMKELNs did not promote the proliferation of hBMSCs under certain concentrations but obviously enhanced the osteogenic differentiation abilities by regulating SOD2. These phenomena may be due to the influence of AMKELNs on the energy metabolism of hBMSCs or related to the oxidative stress response. However, further specific experiments are needed to better elucidate the role of SOD2 in AMKELNs-enhanced osteogenic differentiation of hBMSCs. These should include investigations into glycometabolism, mtROS levels, and the upstream signaling pathways regulating SOD2 [29,48]. In conclusion, clarifying the function of SOD2 in the process where AMKELNs affect the osteogenic differentiation of hBMSCs can provide data reference for developing therapeutic strategies targeting SOD2 to postpone osteoporosis.

It is essential to recognize that AMK is a complicated Chinese medicine comprising diverse bioactive constituents, including sesquiterpenoids, polysaccharides, volatile oils, flavonoids, and phenolic compounds [19]. AMK is well-known for its antioxidant properties. In our investigations, AMKELNs were associated with changes in SOD2 mRNA during the osteogenic differentiation of BMSCs. However, these mechanisms remain incompletely understood. Meanwhile, the specific components in AMKELNs responsible for these effects remain unidentified, posing challenges for clinical trials on bone regeneration and repair. To figure out the effects on hBMSCs' osteogenic differentiation and bone regeneration, it is crucial to identify and purify the contributing substances in AMKELNs and clarify the molecular mechanism. However, the existing extractions of PELNs offer both advantages and disadvantages [59–61]. A delicate balance point needs to be found between output and quality. Gao *et al*. [62] demonstrated the structural diversity, formation mechanisms, and potential functions of extracellular vesicles (EVs) using 3D electron tomography (ET) and immunogold transmission electron microscopy. These results can serve as a reference for further studies of AMKELNs on biogenesis, heterogeneity, and membrane origins. Furthermore, evaluating the relevant indicators, such as the toxicology and pharmacodynamic properties of AMKELNs, is an extremely vital task [63]. The current scarcity of toxicity reports on AMK underscores this need. A safe dosage range needs to be established based on the identified active components, and hepatorenal safety should be evaluated via biochemical indicators [38]. Subsequent work in large-animal models like dogs and horses will be necessary to generate robust preclinical data and support clinical translation [64]. Such investigations are anticipated to advance the development of cell growth factor cocktails with well-defined characteristics for targeted bone tissue engineering.

Despite the encouraging findings of the present study, several limitations should be acknowledged. First, although our data demonstrated that AMKELNs effectively promoted the osteogenic differentiation of hBMSCs and at-

tenuated bone loss in ovariectomized rats, the precise bioactive components responsible for these effects remain to be fully identified. Plant-derived exosome-like nanovesicles are known to exhibit considerable compositional heterogeneity, and their biological activities are likely mediated by a complex interplay of lipids, small RNAs, and proteins. Future studies incorporating component purification strategies and multi-omics analyses, such as lipidomics and small RNA profiling [65–67], will be essential to delineate the key functional cargos of AMKELNs. In addition, bone homeostasis is regulated by highly coordinated interactions among multiple cell populations within the bone microenvironment, including mesenchymal stromal cells, osteoblasts [48], osteoclasts [44], immune cells, and vascular-associated cells. Emerging single-cell and spatial transcriptomic studies [68,69] have highlighted the importance of cellular heterogeneity and lineage-specific responses in skeletal remodeling and osteoporosis progression. Therefore, extending the current findings to cell-type-resolved analyses may provide deeper insight into how AMKELNs modulate the osteogenic niche and oxidative stress responses *in vivo*. Finally, although we identified SOD2 as a critical functional mediator of AMKELN-induced osteogenesis *in vitro*, upstream regulatory mechanisms and *in vivo* molecular validation were not fully addressed in the present study. These aspects represent important avenues for future investigation and will be essential for advancing AMKELNs toward translational applications in osteoporosis therapy.

## Conclusions

In conclusion, our study indicated that AMKELNs isolated from AMK acted as novel promoters of osteogenic differentiation by targeting SOD2. Furthermore, AMKELNs could serve as a potential nanomedicine platform to preserve bone mass and prevent PMOP. These favorable findings could be helpful for developing a new nanomedicine delivery strategy targeting SOD2 for PMOP treatment, which has good potential for clinical translation. Additionally, they can provide valuable insights for investigating the therapeutic potential of spleen-invigorating Chinese medicines for osteoporosis prevention.

## Abbreviations

AMK, *Atractylodes macrocephala Koidz.*; ALP, alkaline phosphatase; Runx2, RUNX family transcription factor 2; OCN, osteocalcin; OPN, osteopontin; OVX, ovariectomized; BMD, bone mineral density; BV/TV, bone volume fraction (bone volume/total volume); Tb.N, trabecular number; Tb.Pf, trabecular bone pattem factor; BCIP/NBT, 5-Bromo-4-chloro-3-indolyl phosphate/nitro blue tetrazolium solution; DAPI, 4′,6-diamidino-2-phenylindole; DiR, 1,1′-Dioctadecyl-3,3,3′,3′-tetramethylindotricarbocyanine iodide; PVDF, Polyvinylidene Fluoride; EDTA, Ethylenediaminetetraacetic Acid; DAB, 3,3′-diaminobenzidine; BMP6, bone morpho- genetic protein 6; SODs, superoxide dismutases; SOD1, superoxide dismutase 1; SOD2, superoxide dismutase 2; SOD3, superoxide dismutase 3; ROS, reactive oxygen species; TEM, transmission electron microscope; qRT-PCR, quantitative reverse transcription polymerase chain reaction; AMKELNs, AMK-derived exosome-like nanovesicles; hBMSCs, human bone marrow-derived mesenchymal stem cells; Micro-CT, micro computed tomography; PMOP, postmenopausal osteoporosis; PBS, phosphate buffered saline; NTA, Nanoparticle Tracking Analysis; FBS, fetal bovine serum; SD, Sprague-Dawley.

## Availability of Data and Materials

The datasets used and/or analyzed during the current study are available from the corresponding author on reasonable request.

## Author Contributions

ZQZ and ZNP designed the research study; WXG collected the bone marrow samples; ZNP, XYW, ZLZ and TYH contributed to the experimental work; XQH, MZD and WQZ provided help and advice on the analysis of transcriptome data and Micro-CT parameters; JQC supervised this study and provided valuable suggestions and revisions; ZQZ wrote the first draft and is responsible for the revision of the article. All authors read and approved the final manuscript for publication. All authors agree to be accountable for all aspects of the research work and ensure that questions related to the accuracy or integrity of any part of the work are appropriately investigated and resolved.

## Ethics Approval and Consent to Participate

The research protocol was approved by the Ethics Committee of Clinical Research of Stem Cells and Somatic Cells of Affiliated Hospital of Guangdong Medical University (Ethic Approval Number: PJGXB2024-001). All animal experiments were approved by Animal Ethical and Welfare Committee of Affiliated Hospital of Guangdong Medical University (approval no. AHGDMU-LAC-B-202405-0024).

## Acknowledgments

We sincerely thank Dr. Peng Li, Dr. Jiafeng Wang, and Ms. Xiang Gao for their thoughtful guidance and help in this study. We also appreciate the Stem Cell Research and Cellular Therapy Center and the Clinical Research Center of Affiliated Hospital of Guangdong Medical University for providing essential equipment.

## Funding

This research was funded by the Affiliated Hospital of Guangdong Medical University “Clinical Medicine+” CnTech Co-construction Platform Foundation (Grant No.

CLP2021A001), and the High-Level Talent Research Start-Up Fund of the Affiliated Hospital of Guangdong Medical University (Grant No. GCC2022014).

## Conflict of Interest

The authors declare no conflict of interest.

## Supplementary Material

Supplementary material associated with this article can be found, in the online version, at https://doi.org/10.22203/eCM.v058a15.

## References

[1] Al Anouti F, Taha Z, Shamim S, Khalaf K, Al Kaabi L, Alsafar H. An insight into the paradigms of osteoporosis: From genetics to biomechanics. Bone Reports. 2019; 11: 100216. https://doi.org/10.1016/j.bonr.2019.100216.

[2] Xiao PL, Cui AY, Hsu CJ, Peng R, Jiang N, Xu XH, *et al*. Global, regional prevalence, and risk factors of osteoporosis according to the World Health Organization diagnostic criteria: a systematic review and meta-analysis. Osteoporosis International: A Journal Established as Result of Cooperation Between the European Foundation for Osteoporosis and the National Osteoporosis Foundation of the USA. 2022; 33: 2137–2153. https://doi.org/10.1007/s00198-022-06454-3.

[3] Reid IR, McClung MR. Osteopenia: a key target for fracture prevention. The Lancet. Diabetes & Endocrinology. 2024; 12: 856–864. https://doi.org/10.1016/s2213-8587(24)00225-0.

[4] Billington E, Aghajafari F, Skulsky E, Kline GA. Bisphosphonates. BMJ: British Medical Journal/British Medical Association. 2024; 386: e076898. https://doi.org/10.1136/bmj-2023-076898.

[5] Palacios S. Medical treatment of osteoporosis. Climacteric: The Journal of the International Menopause Society. 2022; 25: 43–49. https://doi.org/10.1080/13697137.2021.1951697.

[6] Zhu J, Xiong J, Ji W. A Systematic Review of Bone Marrow Stromal Cells and Periosteum-Derived Cells for Bone Regeneration. Tissue Engineering. Part B, Reviews. 2023; 29: 103–122. https://doi.org/10.1089/ten.TEB.2022.0115.

[7] Arthur A, Gronthos S. Clinical Application of Bone Marrow Mesenchymal Stem/Stromal Cells to Repair Skeletal Tissue. International Journal of Molecular Sciences. 2020; 21: 9759. https://doi.org/10.3390/ijms21249759.

[8] Ayub N, Faraj M, Ghatan S, Reijers JAA, Napoli N, Oei L. The Treatment Gap in Osteoporosis. Journal of Clinical Medicine. 2021; 10: 3002. https://doi.org/10.3390/jcm10133002.

[9] Zheng Y, Wang T, Zhang J, Wei S, Wu Z, Li J, *et al*. Plant-Derived Nanovesicles: A Promising Frontier in Tissue Repair and Antiaging. Journal of Agricultural and Food Chemistry. 2025; 73: 13159–13177. https://doi.org/10.1021/acs.jafc.5c01547.

[10] Zeng YB, Deng X, Shen LS, Yang Y, Zhou X, Ye L, *et al*. Advances in plant-derived extracellular vesicles: isolation, composition, and biological functions. Food & Function. 2024; 15: 11319–11341. https://doi.org/10.1039/d4fo04321a.

[11] Kim J, Li S, Zhang S, Wang J. Plant-derived exosome-like nanoparticles and their therapeutic activities. Asian Journal of Pharmaceutical Sciences. 2022; 17: 53–69. https://doi.org/10.1016/j.ajps.2021.05.006.

[12] Ye C, Yan C, Bian SJ, Li XR, Li Y, Wang KX, *et al*. Momordica charantia L.-derived exosome-like nanovesicles stabilize p62 expression to ameliorate doxorubicin cardiotoxicity. Journal of Nanobiotechnology. 2024; 22: 464. https://doi.org/10.1186/s12951-024-02705-z.

[13] Kim J, Gao C, Guo P, Sheng J, Wang J. A novel approach to alleviate acetaminophen-induced hepatotoxicity with hybrid balloon flower root-derived exosome-like nanoparticles (BDEs) with silymarin via inhibition of hepatocyte MAPK pathway and apoptosis. Cell Communication and Signaling: CCS. 2024; 22: 334. https://doi.org/10.1186/s12964-024-01700-z.

[14] Fu J, Liu Z, Feng Z, Huang J, Shi J, Wang K, *et al*. Platycodon grandiflorum exosome-like nanoparticles: the material basis of fresh platycodon grandiflorum optimality and its mechanism in regulating acute lung injury. Journal of Nanobiotechnology. 2025; 23: 270. https://doi.org/10.1186/s12951-025-03331-z.

[15] Yang Y, Yang L, Deng H, Liu Y, Wu J, Yang Y, *et al*. Coptis chinensis-derived extracellular vesicle-like nanoparticles delivered miRNA-5106 suppresses NETs by restoring zinc homeostasis to alleviate colitis. Journal of Nanobiotechnology. 2025; 23: 444. https://doi.org/10.1186/s12951-025-03466-z.

[16] Ye QY, Cui Y, Wang HY, Li LY, Chen JB, Zhu XF, *et al*. Exosomal communication: a pivotal regulator of bone homeostasis and a potential therapeutic target. Frontiers in Pharmacology. 2024; 15: 1516125. https://doi.org/10.3389/fphar.2024.1516125.

[17] Singh K, Singh G, Bhushan B, Kumar S, Dhurandhar Y, Dixit P. A comprehensive pharmacological review of Atractylodes Macrocephala: Traditional uses, phytochemistry, pharmacokinetics, and therapeutic potential. Pharmacological Research-Modern Chinese Medicine. 2024; 10: 100394. https://doi.org/10.1016/j.prmcm.2024.100394.

[18] Yang L, Yu H, Hou A, Man W, Wang S, Zhang J, *et al*. A Review of the Ethnopharmacology, Phytochemistry, Pharmacology, Application, Quality Control, Processing, Toxicology, and Pharmacokinetics of the Dried Rhizome of Atractylodes macrocephala. Frontiers in Pharmacology. 2021; 12: 727154. https://doi.org/10.3389/fphar.2021.727154.

[19] Luo W, Zhang K, Wang Y, Ye M, Zhang Y, Xu W, *et al*. The Rhizome of Atractylodes macrocephala Koidz.: A Comprehensive Review on the Traditional Uses, Phytochemistry and Pharmacology. Chemistry & Biodiversity. 2025; 22: e202401879. https://doi.org/10.1002/cbdv.202401879.

[20] Ha H, An H, Shim KS, Kim T, Lee KJ, Hwang YH, *et al*. Ethanol Extract of Atractylodes macrocephala Protects Bone Loss by Inhibiting Osteoclast Differentiation. Molecules: A Journal of Synthetic Chemistry and Natural Product Chemistry. 2013; 18: 7376–7388. https://doi.org/10.3390/molecules18077376.

[21] Yi G, Zhang R, Li M, Song X, Li S. Atractylenolide-III attenuates osteoarthritis by repolarizing macrophages through inactivating TLR4/NF-κB signaling. International Immunopharmacology. 2024; 129: 111629. https://doi.org/10.1016/j.intimp.2024.111629.

[22] Li X, Wei G, Wang X, Liu DH, Deng RD, Li H, *et al*. Targeting of the Sonic Hedgehog pathway by atractylenolides promotes chondrogenic differentiation of mesenchymal stem cells. Biological & Pharmaceutical Bulletin. 2012; 35: 1328–1335. https://doi.org/10.1248/bpb.b12-00265.

[23] Wang J, Jiang Y, Hou X, Raza T, He Y, Liu X, *et al*. AMP1-1 derived from Atractylodes macrocephala Koidz prevents bone aging triggered by lead and cadmium. Comparative Biochemistry and Physiology. Toxicology & Pharmacology: CBP. 2025; 294: 110189. https://doi.org/10.1016/j.cbpc.2025.110189.

[24] Liu Y, Deng X, Chen C, Fu B, Wang M, Li J, *et al*. Atractylenolide I Attenuates Glucocorticoid-Induced Osteoporosis via Inhibiting NF-κB Signaling Pathway. Calcified Tissue International. 2025; 116: 51. https://doi.org/10.1007/s00223-025-01358-w.

[25] Yu Y, Fu D, Zhou H, Su J, Chen S, Lv G. Potential application of Atractylodes macrocephala Koidz. as a natural drug for bone mass regulation: A review. Journal of Ethnopharmacology. 2023; 315: 116718. https://doi.org/10.1016/j.jep.2023.116718.

[26] Wang Y, Branicky R, Noë A, Hekimi S. Superoxide dismutases: Dual roles in controlling ROS damage and regulating ROS signal-

ing. The Journal of Cell Biology. 2018; 217: 1915–1928. https://doi.org/10.1083/jcb.201708007.

[27] Fujii J, Homma T, Osaki T. Superoxide Radicals in the Execution of Cell Death. Antioxidants. 2022; 11: 501. https://doi.org/10.3390/antiox11030501.

[28] Sahlender B, Windolf J, Suschek CV. Superoxide dismutase and catalase significantly improve the osteogenic differentiation potential of osteogenetically compromised human adipose tissue-derived stromal cells in vitro. Stem Cell Research. 2022; 60: 102708. https://doi.org/10.1016/j.scr.2022.102708.

[29] Qiu W, Sun Q, Li N, Chen Z, Wu H, Chen Z, *et al*. Superoxide dismutase 2 scavenges ROS to promote osteogenic differentiation of human periodontal ligament stem cells by regulating Smad3 in alveolar bone-defective rats. Journal of Periodontology. 2024; 95: 469–482. https://doi.org/10.1002/jper.23-0469.

[30] Zhu B, Zhang QL, Hua JW, Cheng WL, Qin LP. The traditional uses, phytochemistry, and pharmacology of Atractylodes macrocephala Koidz.: A review. Journal of Ethnopharmacology. 2018; 226: 143–167. https://doi.org/10.1016/j.jep.2018.08.023.

[31] Patel D, Wairkar S. Bone regeneration in osteoporosis: opportunities and challenges. Drug Delivery and Translational Research. 2023; 13: 419–432. https://doi.org/10.1007/s13346-022-01222-6.

[32] Wawrzyniak A, Balawender K. Structural and Metabolic Changes in Bone. Animals: An Open Access Journal From MDPI. 2022; 12: 1946. https://doi.org/10.3390/ani12151946.

[33] Price SAL, Finch S, Krejany E, Jiang H, Kale A, Domchek S, *et al*. WHAM—A Prospective Study of Weight and Body Composition After Risk-Reducing Bilateral Salpingo-oophorectomy. The Journal of Clinical Endocrinology and Metabolism. 2023; 109: e397–e405. https://doi.org/10.1210/clinem/dgad385.

[34] Burch KE, McCracken K, Buck DJ, Davis RL, Sloan DK, Curtis KS. Relationship Between Circulating Metabolic Hormones and Their Central Receptors During Ovariectomy-Induced Weight Gain in Rats. Frontiers in Physiology. 2022; 12: 800266. https://doi.org/10.3389/fphys.2021.800266.

[35] Huang F, Gao J, Li A, Mizokami A, Matsuda M, Aoki K, *et al*. Activation of NF-κB signaling regulates ovariectomy-induced bone loss and weight gain. Biochimica et Biophysica Acta. Molecular Basis of Disease. 2024; 1870: 167320. https://doi.org/10.1016/j.bbadis.2024.167320.

[36] Jin Y, Li S, Yu Q, Chen T, Liu D. Application of stem cells in regeneration medicine. MedComm. 2023; 4: e291. https://doi.org/10.1002/mco2.291.

[37] Xia X, Zhu J, Xu X, Wang W, Zhao R, Wu K, *et al*. Current progress of plant-derived exosome-like nanovesicles on the regulation of osteoporosis and osteoarthritis. Annals of Medicine. 2025; 57: 2549524. https://doi.org/10.1080/07853890.2025.2549524.

[38] Hwang JH, Park YS, Kim HS, Kim DH, Lee SH, Lee CH, *et al*. Yam-derived exosome-like nanovesicles stimulate osteoblast formation and prevent osteoporosis in mice. Journal of Controlled Release. 2023; 355: 184–198. https://doi.org/10.1016/j.jconrel.2023.01.071.

[39] Zhan W, Deng M, Huang X, Xie D, Gao X, Chen J, *et al*. Pueraria lobata-derived exosome-like nanovesicles alleviate osteoporosis by enhacning autophagy. Journal of Controlled Release: Official Journal of the Controlled Release Society. 2023; 364: 644–653. https://doi.org/10.1016/j.jconrel.2023.11.020.

[40] Zhao Q, Feng J, Liu F, Liang Q, Xie M, Dong J, *et al*. Rhizoma Drynariae-derived nanovesicles reverse osteoporosis by potentiating osteogenic differentiation of human bone marrow mesenchymal stem cells via targeting ERα signaling. Acta Pharmaceutica Sinica. B. 2024; 14: 2210–2227. https://doi.org/10.1016/j.apsb.2024.02.005.

[41] Liu ZW, Xi XL, Wu TR, Lu YY, Zhong PC, Hu YJ, *et al*. Aikeqing, a kidney- and spleen-tonifying compound Chinese medicine granule, prevented ovariectomy-induced bone loss in rats via the suppression of osteoclastogenesis. Biomedicine & Pharmacotherapy = Biomédecine & Pharmacothérapie. 2023; 166: 115339. https://doi.org/10.1016/j.biopha.2023.115339.

[42] Hua Z, Dai S, Li S, Wang J, Peng H, Rong Y, *et al*. Deciphering the protective effect of Buzhong Yiqi Decoction on osteoporotic fracture through network pharmacology and experimental validation. Journal of Orthopaedic Surgery and Research. 2023; 18: 86. https://doi.org/10.1186/s13018-023-03545-7.

[43] Liang J, Bao AL, Ma HY, Dong W, Li WH, Wu X, *et al*. Prevention of polycystic ovary syndrome and postmenopausal osteoporosis by inhibiting apoptosis with Shenling Baizhu powder compound. PeerJ. 2022; 10: e13939. https://doi.org/10.7717/peerj.13939.

[44] Lee SH, Kim SJ, Kim SJ. Anti-oxidant activity with inhibition of osteoclastogenesis by Atractylodes Rhizoma extract. Eurpean Review for Medical and Pharmacological Sciences. 2014; 18: 1806–1812. Available at: https://www.europeanreview.org/article/7536 (Accessed: 21 May 2004).

[45] Xie S, Zou W, Liu S, Yang Q, Hu T, Zhu WP, *et al*. Site 1 protease aggravates acute kidney injury by promoting tubular epithelial cell ferroptosis through SIRT3-SOD2-mtROS signaling. The FEBS Journal. 2024; 291: 1575–1592. https://doi.org/10.1111/febs.17057.

[46] Wang HQ, Zhu YW, Dou ZY, Chen Z, Tong CC, He X, *et al*. 1,25(OH)(2)D(3) Ameliorates DSS-induced Intestinal Ferroptosis through the SIRT3-SOD2-mtROS Pathway. The Journal of Nutritional Biochemistry. 2025; 144: 109999. https://doi.org/10.1016/j.jnutbio.2025.109999.

[47] Schoppa AM, Chen X, Ramge JM, Vikman A, Fischer V, Haffner-Luntzer M, *et al*. Osteoblast lineage Sod2 deficiency leads to an osteoporosis-like phenotype in mice. Disease Models & Mechanisms. 2022; 15: dmm049392. https://doi.org/10.1242/dmm.049392.

[48] Gao J, Feng Z, Wang X, Zeng M, Liu J, Han S, *et al*. SIRT3/SOD2 maintains osteoblast differentiation and bone formation by regulating mitochondrial stress. Cell Death and Differentiation. 2018; 25: 229–240. https://doi.org/10.1038/cdd.2017.144.

[49] Li Y, Wang T, Li X, Li W, Lei Y, Shang Q, *et al*. SOD2 promotes the immunosuppressive function of mesenchymal stem cells at the expense of adipocyte differentiation. Molecular Therapy: The Journal of the American Society of Gene Therapy. 2024; 32: 1144–1157. https://doi.org/10.1016/j.ymthe.2024.01.031.

[50] Li H, Li T, Wang S, Wei J, Fan J, Li J, *et al*. miR-17-5p and miR-106a are involved in the balance between osteogenic and adipogenic differentiation of adipose-derived mesenchymal stem cells. Stem Cell Research. 2013; 10: 313–324. https://doi.org/10.1016/j.scr.2012.11.007.

[51] Gao JW, Song MK, Wu DZ, Yan T, Zhao K, Huang YS, *et al*. CircRBM23 regulates the switch between osteogenesis and adipogenesis of mesenchymal stem cells via sponging miR-338-3p. Clinical Science. 2023; 137: 495–510. https://doi.org/10.1042/cs20220833.

[52] Ren L, Zhu X, Tan J, Lv X, Wang J, Hua F. MiR-210 promotes bone formation in ovariectomized rats by regulating osteogenic/adipogenic differentiation of bone marrow mesenchymal stem cells through downregulation of EPHA2. Journal of Orthopaedic Surgery and Research. 2023; 18: 811. https://doi.org/10.1186/s13018-023-04213-6.

[53] Hu L, Yin C, Zhao F, Ali A, Ma J, Qian A. Mesenchymal Stem Cells: Cell Fate Decision to Osteoblast or Adipocyte and Application in Osteoporosis Treatment. International Journal of Molecular Sciences. 2018; 19: 360. https://doi.org/10.3390/ijms19020360.

[54] Ding Y, Yang H, Wang Y, Chen J, Ji Z, Sun H. Sirtuin 3 is required for osteogenic differentiation through maintenance of PGC-1α-SOD2-mediated regulation of mitochondrial function. International Journal of Biological Sciences. 2017; 13: 254–264. https://doi.org/10.7150/ijbs.17053.

[55] Chen CT, Shih YR, Kuo TK, Lee OK, Wei YH. Coordinated Changes of Mitochondrial Biogenesis and Antioxidant Enzymes During Osteogenic Differentiation of Human Mesenchymal Stem Cells. Stem Cells. 2008; 26: 960–968. https://doi.org/10.1634/stemcells.2007-0509.

[56] Nolfi-Donegan D, Braganza A, Shiva S. Mitochondrial electron transport chain: Oxidative phosphorylation, oxidant production, and methods of measurement. Redox Biology. 2020; 37: 101674. https://doi.org/10.1016/j.redox.2020.101674.

[57] Li B, Ming H, Qin S, Nice EC, Dong J, Du Z, *et al*. Redox regulation: mechanisms, biology and therapeutic targets in diseases. Signal Transduction and Targeted Therapy. 2025; 10: 72. https://doi.org/10.1038/s41392-024-02095-6.

[58] Candas D, Li JJ. MnSOD in oxidative stress response-potential regulation via mitochondrial protein influx. Antioxidants & Redox Signaling. 2014; 20: 1599–1617. https://doi.org/10.1089/ars.2013.5305.

[59] Calzoni E, Cusumano G, Bertoldi A, Alabed HBR, Pellegrino RM, Buratta S, *et al*. Rhubarb-Derived Extracellular Vesicles Mitigate Oxidative Stress and Metabolic Dysfunction in an Alzheimer's Cellular Model. Nutrients. 2025; 17: 3771. https://doi.org/10.3390/nu17233771.

[60] Huang J, Feng Z, Fu J, Zou J, Xiang Q, Liu X, *et al*. Amelioration of acute lung injury by Salvia miltiorrhiza-derived extracellular vesicles: through repair of the vascular barrier and modulation of lung microbiota. Chinese Medicine. 2026; 21: 6. https://doi.org/10.1186/s13020-025-01203-0.

[61] Sarwareddy KK, Singh AD, Patnam S, Sesuraj BA, Ponamgi S, Thakur BK, *et al*. Harnessing tomato-derived small extracellular vesicles as drug delivery system for cancer therapy. Future Science OA. 2025; 11: 2461956. https://doi.org/10.1080/20565623.2025.2461956.

[62] Gao J, Li Y, Zhang S, He Y, Liu Z, Wang J, *et al*. Structural and Functional Characterization of EXPO-Derived Extracellular Vesicles in Plants. Advanced Science. 2026, 13: e06163. https://doi.org/10.1002/advs.202506163.

[63] Zhang J, Pang H, Tang H, Tu Q, Xia F, Zhang H, *et al*. The pharmacodynamic and pharmacological mechanisms underlying nanovesicles of natural products: Developments and challenges. Pharmacology & Therapeutics. 2025; 265: 108754. https://doi.org/10.1016/j.pharmthera.2024.108754.

[64] O'Brien TJ, Hollinshead F, Goodrich LR. Extracellular vesicles in the treatment and prevention of osteoarthritis: can horses help us translate this therapy to humans? Extracellular Vesicles and Circulating Nucleic Acids. 2023; 4: 151–169. http://doi.org/10.20517/evcna.2023.11.

[65] Hao S, Hua Z, Yuan Y. Stage-Specific Lipidomes of Gastrodia elata Extracellular Vesicles Modulate Fungal Symbiosis. International Journal of Molecular Sciences. 2025; 26: 8611. https://doi.org/10.3390/ijms26178611.

[66] Zanotti C, Troise AD, Arena S, Renzone G, De Pascale S, Ferracane R, *et al*. Isolation of Red Beet Plant-Derived Nanovesicles, and Characterization of Their Molecular Content and Biological Activities in Human Cells. International Journal of Molecular Sciences. 2025; 26: 11261. https://doi.org/10.3390/ijms262311261.

[67] Ming T, Yang Y, Zhu J, Lin J, Yang W, Yu G, *et al*. Ginger-Derived Exosome-Like Nanoparticles: The Effect of Extraction Methods on Metabolites and in vitro Anti-Lung Cancer Activity. International Journal of Nanomedicine. 2025; 20: 13399–13420. https://doi.org/10.2147/ijn.S541948.

[68] Guo Q, Wang Q, Chen J, Zhao M, Lu T, Guo Z, *et al*. Dihydroartemisinin Regulated the MMP-Mediated Cellular Microenvironment to Alleviate Rheumatoid Arthritis. Research: A Science Partner Journal. 2024; 7: 0459. https://doi.org/10.34133/research.0459.

[69] Qi W, Yang L, Pan Y, Lv K, Zhao L, Zhang Y, *et al*. Chinese leek-derived extracellular vesicles ameliorate sarcopenia by regulating mitochondrial biogenesis and autophagy via AMPK and maintaining myosin homeostasis. Journal of Nanobiotechnology. 2025; 23: 721. https://doi.org/10.1186/s12951-025-03764-6.

**Editor's note**: The Scientific Editors responsible for this paper were Fergal J. O'Brien and Kelong Fan.

**Received**: 3rd July 2025; **Accepted**: 1st June 2026; **Published**: 31st August 2026